Rigorous control of vesicle-forming lipid pKa by fluorine-conjugated bioisosteres for gene-silencing with siRNA

Ayaka Okamoto, Hiroyuki Koide, Naoki Morita, Yusuke Hirai, Yuji Kawato, Hiromichi Egami, Yoshitaka Hamashima, Tomohiro Asai, Takehisa Dewa, Naoto Oku

PII: S0168-3659(18)30749-1
DOI: https://doi.org/10.1016/j.jconrel.2018.12.044
Reference: COREL 9594

To appear in: *Journal of Controlled Release*

Received date: 12 October 2018
Revised date: 8 December 2018
Accepted date: 25 December 2018

Please cite this article as: Ayaka Okamoto, Hiroyuki Koide, Naoki Morita, Yusuke Hirai, Yuji Kawato, Hiromichi Egami, Yoshitaka Hamashima, Tomohiro Asai, Takehisa Dewa, Naoto Oku , Rigorous control of vesicle-forming lipid pKa by fluorine-conjugated bioisosteres for gene-silencing with siRNA. Corel (2018), https://doi.org/10.1016/j.jconrel.2018.12.044

Rigorous control of vesicle-forming lipid pK_a by fluorine-conjugated bioisosteres for gene-silencing with siRNA

Ayaka Okamoto [a], Hiroyuki Koide [a], Naoki Morita [b], Yusuke Hirai [a], Yuji Kawato [b], Hiromichi Egami [b], Yoshitaka Hamashima [b], Tomohiro Asai [a], Takehisa Dewa [c], and Naoto Oku [a,*]

Department of [a]Medical Biochemistry and [b]Synthetic Organic Chemistry, School of Pharmaceutical Sciences, University of Shizuoka, 52-1 Yada, Suruga-ku, Shizuoka 422-8526, Japan

[c]*Department of Life Science and Applied Chemistry, Nagoya Institute of Technology, Gokiso-cho, Showa-ku, Nagoya 466-8555, Japan*

*Corresponding author. Tel: +81 54 264 5701, Fax: +81 54 264 5705.

E-mail address: oku@u-shizuoka-ken.ac.jp. (N. Oku)

Graphical Abstract

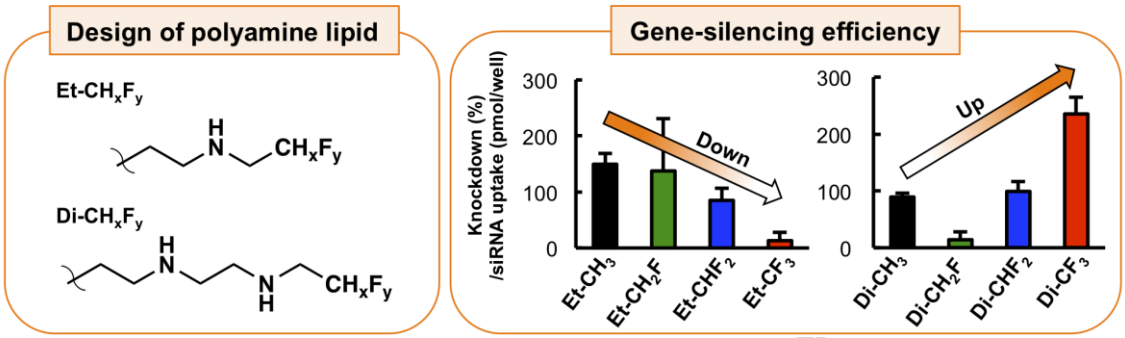

Abstract

While the influence of pK_a provided by amine-containing materials in siRNA delivery vectors for use in gene-silencing has been widely studied, there are little reports in which amine pK_a is controlled rigorously by using bioisosteres and its effect on gene-silencing. Here, we report that amine pK_a could be rigorously controlled by replacement of hydrogen atom(s) with fluorine atom(s). A series of mono- and di-amine lipids with a different number of fluorine atoms were synthesized. The pK_a of the polyamine lipids was shifted to a lower value with an increase in the number of fluorine atoms. The optimal pK_a for high gene-silencing efficiency varied according to the number of amine residues in the polyamine lipid. Whereas the endosomal escape ability of mono-amine lipid-containing lipid vesicles (LVs) depended on the pK_a, that of all tested di-amine lipid-containing LVs showed equal membrane-destabilizing activity. LVs showing moderately weak interactions with siRNA facilitated cytoplasmic release of siRNA, resulting in strong gene-silencing. These findings indicate that appropriate amine pK_a engineering depending on the number of amines is important for the induction of effective RNA interference.

KEYWORDS:lipid nanoparticle, siRNA, p*K*a, fluorine

1. Introduction

Pharmaceuticals such as small-molecule and biomedical drugs have made great contribution to longevity. However, there are many diseases untreatable by these pharmaceuticals [1,2]. Oligonucleotides such as antisense, siRNA and miRNA have received much interest as novel therapeutic agents capable of treating such diseases, because they specifically lead to cleavage or functional inhibition of their target mRNA[3] and can be designed and synthesized according to the sequence on demand. As certain types of oligonucleotides act in the cytoplasm, they face several hurdles to get there: 1) being taken up into cell, 2) escaping from the endosomes, and 3) being released into the cytoplasm [4]. Unfortunately, the physicochemical properties of oligonucleotides such as their high molecular weight, hydrophilicity, and high negative-charge density make it difficult for them to break these barriers by themselves. In addition, oligonucleotides are decomposed by nucleases and eliminated rapidly after entrance into the bloodstream [5]. Therefore, various materials such as liposomes [6], lipid nanoparticles [7], polymer nanoparticles [8], dendrimers [9], and nanogels [10] have been studied widely as their carriers.

Polyethylenimine (PEI) has been widely used as a polycationic material for the holding of oligonucleotides such as siRNAs in the carriers. Although transfection with siRNA in PEI-containing nanocarriers results in a significant gene-silencing effect by increasing siRNA uptake into the cell and providing endosomal escape ability [11], its strong cytotoxicity has been a critical problem [12]. Therefore, a number of studies have been carried out to reduce the toxicity and enhance the knockdown effect by improving polycation structure. For example, Kataoka's group prepared a series of the *N*-substituted polyaspartamides possessing repeating aminoethylene units [13]; Hope's group synthesized 56 kinds of amino lipids that include primary, secondly or tertiary amine residues [14]; Anderson's group prepared a large library of lipidoids containing a secondary or a tertiary amine residue [15]; Harashima's group synthesized dimethylamino lipids containing different numbers of methylene units [16]; and Siegwart's group synthesized 139 lipocationic polyesters containing dialkyl amine or heterocyclic amine polymer [17]. These reports indicate that amine pK_a (pK_a = 6.2–6.5) is important for efficient gene-silencing and reduced cytotoxicity. However, precise

regulation of the amine pK_a without a significant change in the chemical structure is considered to be extremely difficult, since adjustment of the amine pK_a usually requires conjugation with bulky groups such as alkyl chain, benzene, cycloalkane or bicyclo-compound to the amine group [14-17]. These modification changes the steric bulk of the molecules along with the pK_a. It is known that steric bulk has a significant effect on gene-silencing [15]. Therefore, rigorous control of amine pK_a without drastic structural change, and investigation of the amine pK_a influence on gene-silencing is still a great challenge and important for the designing of siRNA carriers.

In the present study, we focused on the use of fluorine atoms for rigorous control of amine pK_a. As the fluorine atom is a strong electron-withdrawing substituent and has an atomic size similar to that of hydrogen [18], the pK_as of conjugate acids derived from neighboring nitrogen atoms decrease in accordance with the number of fluorine atoms without causing a significant change in chemical structure or steric bulk [19]. We used ethylenediamine (EtDA) as a model amine group. In addition, diethylenetriamine (DiETA) was used to examine the effect of the number of amines on the gene-silencing.

2. Material and methods

2.1 Titration of polyamine lipid

Preparation procedures for DCP-polyamine-CH_2R (Et-CH_3, Et-CH_2F, Et-CHF_2, Et-CF_3, Di-CH_3, Di-CH_2F, Di-CHF_2 and Di-CF_3) were described in Supporting Information. DCP-polyamine-CH_2R and DSPE-PEG2000 (1/0.1 as a molar ratio) were dissolved in *t*-butanol and lyophilized. Liposomes were produced by hydration of the lipid mixture with RNase-free water. The liposomes were diluted (final lipid conc.: 2 mM) with 5 mL of ultra pure water containing 150 mM NaCl, and basified with 0.1 M NaOH. Five µL of 0.1 M HCl was added to the vial by use of micropipette while stering the solution. pH change was monitored by use of pH meter HM-31P (DKK-TOA, Tokyo, Japan). After stabilized the pH, additional HCl was dropped.

2.2 Preparation of lipid vesicles

DOPE, Cholesterol, DPPC and polyamine lipid (1/1/0.5/0.5 as a molar ratio) were dissolved in *t*-butanol and lyophilized. Lipid vesicles (LVs) were produced by hydrating the lipid mixture with RNase-free water. LVs were freeze-thawed 3-times to prepare unilamellar vesicles.

2.3 TNS assay

Ten µL of 1 mM LVs were diluted in 480 µL of assay buffer containing 20 mM sodium phosphate, 25 mM citrate, 20 mM ammonium acetate, 150 mM NaCl (pH 2.0-12.0), and incubated for 20 min at room temperature. Then, 10 µL of 0.3 mM TNS in was mixed with the LVs solutions. The fluorescence intensity of TNS was determined with a Tecan Infinite M200 microplate reader (Salzburg, Austria) operated according to the manufacturer's instructions (ex. 322 nm, em. 431 nm).

2.4 Preparation of siRNA-encapsulated LVs

siRNA-encapsulated lipid vesicles (sLVs) was prepared by freeze-thawing of siRNA and LVs complex as described previously [21]. LVs and siRNA were mixed (protonable amine groups in polyamine lipid / phosphorus atoms in siRNA = 20 as a molar ratio) and incubated for 20 min at room temperature in 1 mM citric acid/RNase-free water (pH 3.0) to form siRNA/LVs complexes. Then, the complex was frozen in liquid nitrogen and thawed in a water bath at 45°C with vortexing to prepare sLVs. Cell-penetrating peptides (CPP)-DOPE conjugate (6 mol% to total lipids) was modified to sLVs by incubating them at 50°C for 30 min (sLVs-CPP). The amino acid sequence of CPP is RRRRRRGGRRRRG.

2.5 Cell culture

HT1080 human fibroblast cells and HT1080 expressing enhanced green fluorescent protein (HT1080-EGFP) cells were cultured with D-MEM/Ham's F-12 containing 10% fetal bovine serum, 100-units/mL penicillin G and 100-μg/mL streptomycin in a CO_2 incubator.

2.6 siRNA transfection

Cells were seeded onto a culture plate and pre-cultured overnight. The medium was changed to a fresh one supplemented with FBS and free of antibiotics (adjusted pH 7.4) before transfection. Et-sLVs-CPP or Di-sLVs-CPP was added to the culture medium, and the cells were then incubated for 24 h at 37°C in a 5% CO_2 incubator. After a medium change, the cells were incubated for the desired time as described for each experimental procedure.

2.7 siRNA uptake test

HT1080 cells were seeded onto 24-well plates (BD Bioscience, San Jose, CA)

at the density of 1.5×10^4 cells/well. FITC-labeled siRNA formulated in LVs-CPP were added to the cells (5 pmol/500 μL; 10 nM as siRNA) and incubated for 24 h. After having been washed with PBS containing 30 units/mL heparin, the cells were lysed with 1 w/v% *n*-octyl-*β*-D-glucoside containing the following protease inhibitors: 1 mM phenylmethylsulfonyl fluoride, 2 μg/mL leupeptin, 2 μg/mL aprotinin, and 2 μg/mL pepstatin A. The fluorescence intensity of FITC was determined with a Tecan Infinite M200 microplate reader (ex. 495 nm, em. 535 nm). Total protein contents were measured by bicinchoninic acid assay using a Pierce™ BCA Protein Assay Reagent Kit according to the manufacturer's instructions.

2.8 Gene-silencing effect

HT1080-EGFP cells (1.5×10^4 cells/well) were seeded onto 24-well plates (BD Bioscience) and transfected with siRNA against GFP (siGFP) formulated in each LVs-CPP for 24 h at a final siGFP concentration of 10 nM (5 pmol/500 μL). After the medium had been changed to a fresh one, the cells were cultured for an additional 48 h. Cell viability was determined by WST-8 assay; the media was changed to WST-8 assay reagent (Cell Counting Kit-8 : medium = 7.5 μL : 292.5 μL), and then the cells were incubated for 1 h at 37°C. To determine cell viability, absorbance of supernatant at 450 nm was measured using Tecan Infinite M200 microplate reader. Then, the cells were washed with PBS and lysed with 1 w/v% *n*-octyl-*β*-D-glucoside containing the protease inhibitors. Gene silencing against EGFP was determined as a reduction rate of the fluorescence intensity measured with a Tecan Infinite M200 microplate reader (ex. 485 nm, em. 535 nm). Total protein content measured with a Pierce™ BCA Protein Assay Reagent Kit. RNA interference efficiency was determined as follows: Knockdown (%) / siRNA uptake (pmol/well).

2.9 Hemolysis assay

For preparation of erythrocyte, 500 μL of caw blood was washed by gently vortexing with 1 mL of PBS, and was centrifuged at 10,000 x*g* for 10 min at 4°C. After

repeating the wash with PBS five times, the pellet was suspended with 0.3 M sucrose in ultra-pure water. sLVs-CPP diluted with 10 mM phosphate buffer (pH 7.4 or 5.5) containing 0.3 M sucrose were mixed with 10 μL of the erythrocyte (100 μM as amine moiety), and incubated at 37°C for 1 h in a shaking container. After centrifugation (10,000 x*g* for 10 min at room temperature), the liberated hemoglobin was determined by colorimetric analysis of the supernatant at 405 nm with a Tecan Infinite M200 microplate reader. The value for 100% hemolysis was set from the erythrocytes treated with 0.1% Triton X-100. The ζ-potential of the sLVs-CPP diluted with 10 mM phosphate buffer (pH = 5.5 or 7.4) was measured by use of Zetasizer Nano ZS (Malvern).

2.10 Isothermal titration calorimetric assay

Isothermal titration calorimetry was performed with MicroCal PEAQ-ITC (Malvern) at 25°C. Injection cell was filled with 300 nM siRNA solution in 1 mM phosphate buffer (pH 7.4 or 5.5). Et-LVs or Di-LVs was titrated into the cell according to the manufacturer's program. Data was analyzed by use of the MicroCal PEAQ-ITC Analysis (Malvern).

2.11 Confocal laser-scanning microscopy

HT1080 cells were seeded onto glass bottom 24-well plate (AGC Techno Glass Co., Ltd., Shizuoka, Japan) at a density of 1.5×10^4 cells/well. FITC-labeled siRNA-encapsulating Et-LVs-CPP or Di-LVs-CPP was added to the cells (siRNA concentration was 10 nM; 5 pmol/500 μL/well). Distribution of FITC-labeled siRNA in the HT1080 cells was observed under an A1R$^+$ confocal laser-scanning microscope (Nikon, Tokyo, Japan). Individual cells within a single field of view were imaged every 5 min for 24 h. siRNA diffusion time after transfection of LVs-CPP and the proportion of siRNA-diffusing cell at selected time points were determined. The proportion of siRNA-diffusing cells was calculated as follows: the number of FITC-distributed cells / the number of all the cells.

2.12 Statistical analysis

Differences within a group were evaluated by analysis of variance (ANOVA) with the Tukey *post-hoc* test.

3. Results and discussion

3.1 Rigorous control of amine pKa by replacement of hydrogen atom(s) with fluorine atom(s).

Procedures for the synthesis of dicetylphosphate (DCP)-EtDA and -DiETA are shown in **Figure 1**. As for (DCP)-EtDA-CH_2R (R indicates CH_3 ([**Et-CH_3**], CH_2F ([**Et-CH_2F**]), CHF_2 ([**Et-CHF_2**], CF_3 [**Et-CF_3**]), reductive amination of the corresponding fluorine-containing primary amines with *N*-Boc-2-aminoacetaldehyde (**a**) was first conducted. Removal of the Boc protection with 4 M HCl proceeded smoothly to furnish the diamine backbone. Fortunately, in line with our previous reports [6], the amidation with dicetyl chlorophosphate (**b**) occurred chemoselectively at the primary amine under typical conditions. Though a tedious reaction sequence was required, a similar method was applicable for the synthesis of (DCP)-DiETA-CH_2R (**Di-CH_3**, **Di-CH_2F**, **Di-CHF_2**, **Di-CF_3**, respectively). Initially, with the same amines as a starting material, *N*-Boc-*N*-fluoroalkyl-2-aminoacetal-dehydes were prepared through a reaction set consisting of reductive amination with (*tert*-butyldimethylsiloxy)a-cetaldehyde (**c**), Boc protection, and desilylation followed by oxidation of the primary alcohol. Requisite elongation to the triamine backbone was readily performed with *N*-Boc-ethylenediamine (**d**), and the resulting primary amine was conjugated to chlorophosphate.

To determine the pK_a of the lipids, acid-base titration was performed with 0.1 M HCl. While the titration curves of EtDA-lipids showed a single equivalence point and DiETA-lipids showed a two-phase equivalence curve (**Figure S1**), the pK_a of EtDA-lipids was gently shifted to lower value by increasing the number of fluorine atoms (**Table 1**). In addition, both pK_{a1} and pK_{a2} of DiETA-lipids were also shifted to lower values in response to the substitution with fluorine. The pK_a of **Et-CF_3** and pK_{a2} of **Di-CF_3** could not be determined due to loss of buffering capacity over the range of pH 2–11. From these results, we succeeded in rigorous control of amine pK_a by fluorine substitution without causing any significant change in chemical structure or steric bulk.

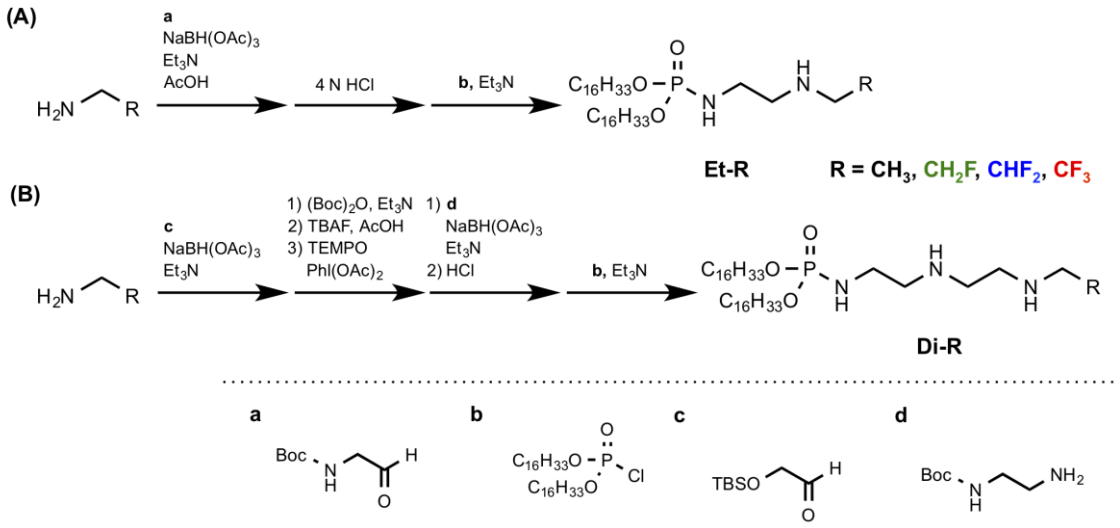

Figure 1. Synthesis of fluorine-conjugated lipids.

(A) Dicetylphosphate-ethylenediamine-CH_2R (Et-R) and (B) Dicetylphosphate-diethylenetriamine-CH_2R (Di-R) conjugates were synthesized by reductive amination.

Table 1. pK_a values of polyamine lipids

	pK_{a1}	pK_{a2}		pK_{a1}	pK_{a2}
Et-CH_3	8.2	-	Di-CH_3	9.2	5.4
Et-CH_2F	5.3	-	Di-CH_2F	8.0	4.9
Et-CHF_2	4.4	-	Di-CHF_2	7.5	3.9
Et-CF_3	< 3.3	-	Di-CF_3	7.1	< 3.0

3.2 Effect of the number of amines and fluorine atoms on gene-silencing

We next prepared lipid vesicles (LVs) composed of dioleoylphosphatidylethanolamine (DOPE), cholesterol, dipalmitoylphosphatidylcholine (DPPC), and EtDA-lipid or DiETA-lipid (Et-LVs, Di-LVs, 1/1/0.5/0.5 as a molar ratio). Charged percentage of the LVs within the pH 2–12 range was measured by using 6-(*p*-toluidino)-2-naphthalenesulfonic acid [20]. Although the curve of Et-LVs shifted to low pH side by increasing the number of fluorine atom, that of Di-LVs did not show any considerable change (**Figure 2A**). These results suggest that the surface charge of mono-amine-containing nanoparticles depended on the pK_a of the amino group whereas that of di- or more amine-containing nanoparticles did not depend on the amine pK_a

To evaluate the gene-silencing activity of siRNA delivered with these LVs, we prepared siRNA-encapsulated LVs (sLVs) by freeze-thawing siRNA and LV complexes 3 times in 1 mM citric acid (pH 3.0, **Figure S2**) [21]. In this study, FITC-conjugated siRNA was used for the uptake test, and siRNA against green fluorescent protein (GFP) was used for the gene-silencing assay. Importantly, un-encapsulated siRNA was not detected by performing an electrophoretic assay after the freeze-thawing (**Figure S3**). Modification of functional peptides has often been used to improve cellular uptake of nanocarriers [22]. In the present study, we modified the sLV surface with cell-penetrating peptide (CPP) [23] (sLV-CPP, **Figure S3**). Then, the cellular uptake ratio and gene-silencing effect of each sLV-CPP were examined (**Figure 2B**, **Figure S4**-**S6**). No cytotoxicity was observed with any sLV-CPP (**Figure S6**). Surprisingly, the optimal amine pK_a for a high knockdown effect depended on the number of amines. Thus, sLV-CPP containing **Et-CH$_3$** (pK_a = 8.2) showed a high knockdown effect in the EtDA (mono-amine) group; and sLV-CPP containing **Di-CF$_3$**, (pK_{a1} = 7.1, pK_{a2} < 3.0) in the DiETA (di-amine) group. These results indicate that the balance between the number of amines and fluorine atoms was crucial to achieve the high knockdown effect.

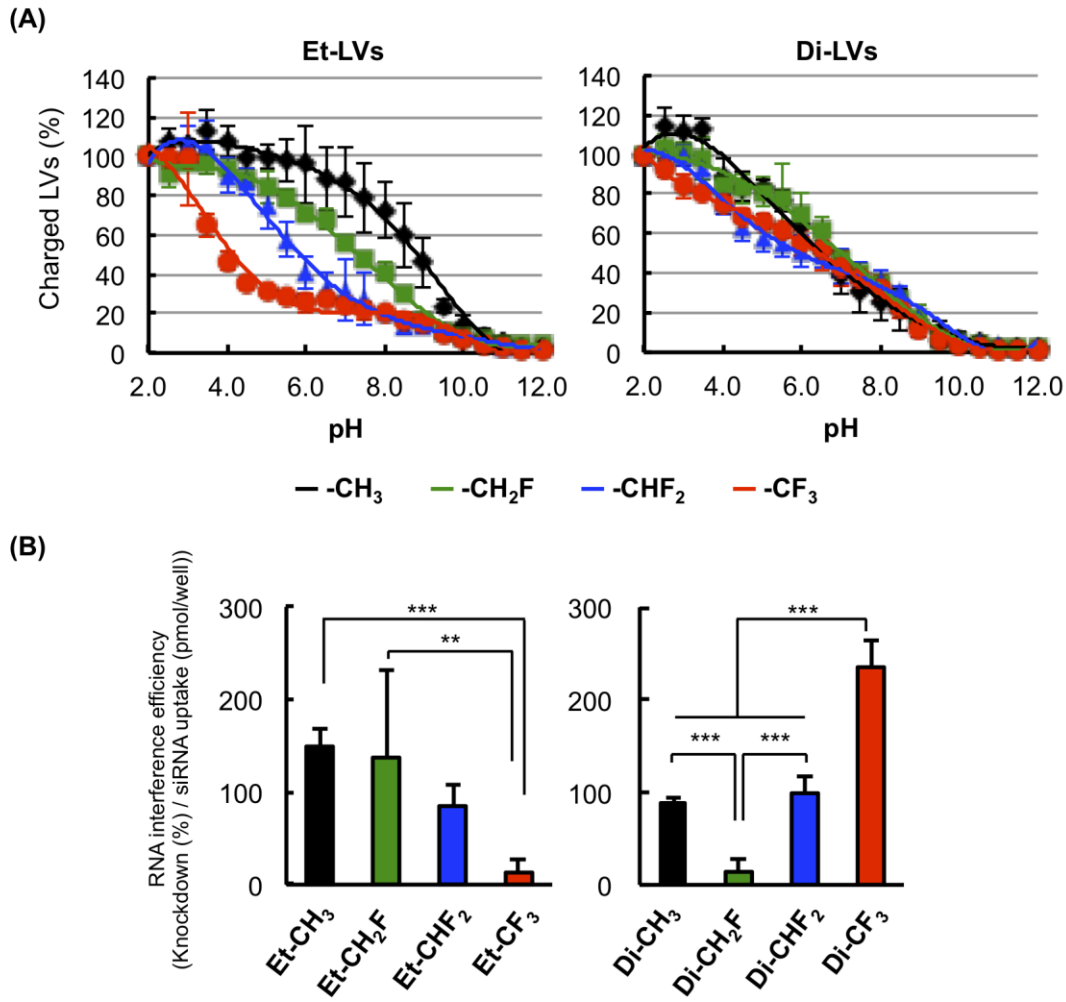

Figure 2. Effect of the number of amines and fluorine atoms on gene-silencing.

(A) TNS was mixed with lipid vesicles in a series of buffers with pH ranging between 2 and 12. Fluorescence intensity was normalized by the TNS fluorescence value at pH 2.0. (B) HT1080-EGFP cells were transfected with siGFP-encapsulating LV-CPP. RNA interference efficiency was determined as follows: Knockdown (%) / siRNA uptake (pmol/well). Significant differences :***P*<0.01, ****P*<0.001

3.3 Endosomal escape ability of sLV-CPP

It is known that the ability to escape endosomes is important for gene-silencing induction [24]. Hemolysis assay is known as a surrogate assay to test for endosomal escape ability because of similarities in their lipid bilayer and glycocalyx compositions [25]. As endosomal pH is known to decrease with endosome maturation [26], caw erythrocytes were incubated with each sLV-CPP in 10 mM phosphate buffer adjusted pH at 5.5 or at 7.4 for 1 h (**Figure 3A**). The pH-responsive hemolytic activity was observed with both Et- and Di-sLV-CPP. The hemolytic activity decreased as the pK_a in the Et-sLV-CPP decreased. It is known that positively charged nanoparticles tend to induce strong hemolytic activity [27]. Since the surface charge of Et-sLV-CPP decreased with increasing fluorine number (**Figure 3B**), the hemolytic activity should also be decreased accordingly. These results indicate that **Et-CHF_2**- and **Et-CF_3**-sLVs could not break the endosomal membrane even if the endosome was acidified. Then, the siRNA should remain in the endosome and be enzymatically degraded [28]. Importantly, pH-dependent change of ζ-potentials of sLVs-CPP was similar to sLVs (without CPP modification). In contrast, there was no correlation between the number of fluorine atoms and the hemolytic activity of Di-sLV-CPP. This data is following the result that Di-sLVs-CPPs have similarly charged percentage and the surface charges. Surface charges of Di-sLVs-CPP were not significantly changed even if increasing of fluorine atom number because pK_{a2} is still above 5.5 (**Figure 3B**). Therefore, hemolytic activities of Di-sLVs-CPP were not changed with the fluorine atom number unlike Et-sLVs. The data suggest that the impact of pK_a on membrane-destabilizing activity was small in the di- or more-amine-containing LVs.

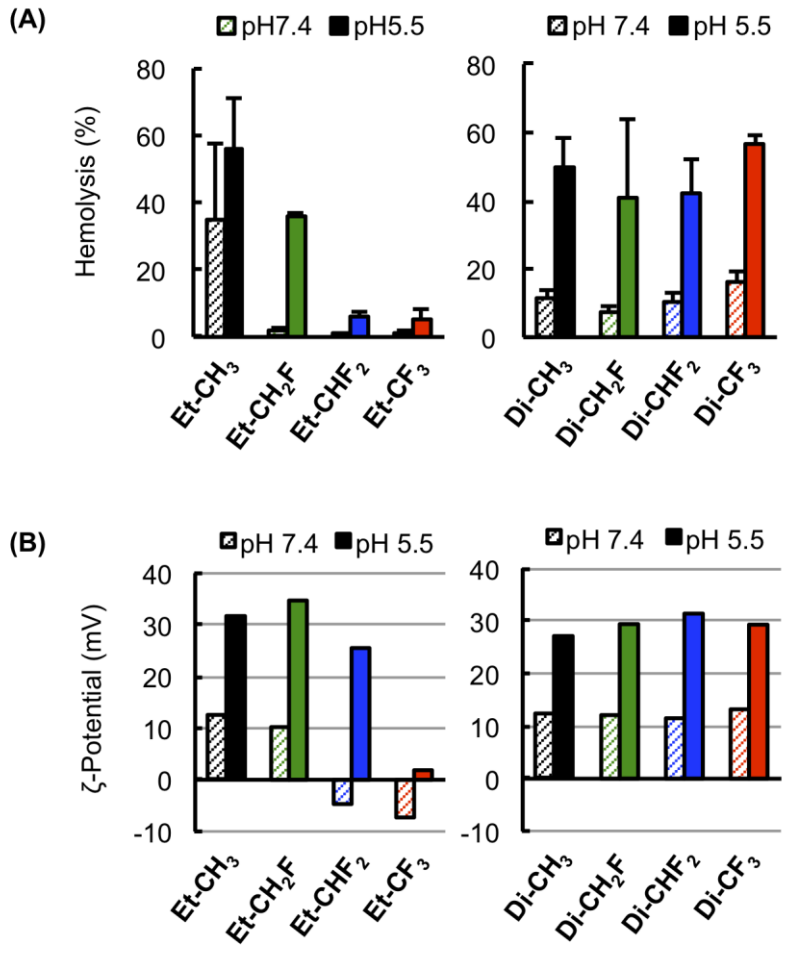

Figure 3. Membrane-destabilizing activity of sLVs-CPP.

(A) sLVs-CPP were incubated with RBCs at 37°C for 1 h in 10 mM phosphate buffer containing 0.3 M sucrose at pH 7.4 or 5.5. After centrifugation, absorbance of leaked-hemoglobin was determined at 405 nm. (B) The ζ-potential of each sLVs-CPP in 10 mM phosphate buffer was measured. Bars with oblique line indicate the ζ-potentials of sLVs-CPP at pH 7.4. Filled bars indicate those at pH 5.5.

3.4 Effect of binding affinity of Di-LVs for siRNA on gene-silencing

We next measured the binding affinity of siRNA for LVs. siRNA needs to form RISC in the cytoplasm after the endosomal escape for gene-silencing. Therefore, effective hand-off of siRNA from LVs to the RISC should be important for a strong gene-silencing effect. We hypothesized that binding affinity of siRNA for **Di-CF_3**-LVs, which showed a strong gene-silencing effect, would be weak in the cytoplasm compared with that of other Di-LVs. Apparent dissociation equilibrium constants (K_d) of siRNA for LVs were measured by isothermal titration calorimetry (**Figure S7**, **Table 2**). The K_d of **Et-CH_3**- or **Et-CH_2F**-LVs at pH 7.4 was 1.27 μM or 2.43 μM, respectivery. The K_d of **Et-CHF_2**- and **Et-CF_3**-LVs were unable to determine. siRNA showed stronger binding affinity for all Di-LVs at pH 5.5 than at pH 7.4, due to their positive charge at pH 5.5 (**Figure 2A**, **3B**). The K_d values of **Di-CH_3**-, **Di-CH_2F**-, or **Di-CHF_2**-LVs were in the range of 100–500 nM at pH 7.4. In contrast, the K_d of **Di-CF_3**-LVs was 3–10 times larger (1.57 μM) than that of other Di-LVs. Since the pK_a of **Di-CF_3** is lower than that of other Di-lipids, the amine of the **Di-CF_3**-LVs should be less protonated than that of the other Di-LVs at pH 7.4. As described above, each Di-LVs had equal hemolytic activity (**Figure 3A**). Therefore, the weak interaction of siRNA with LVs in the cytoplasm should be an important for the release of siRNA from LVs, resulting in strong gene-silencing. In fact, the K_d of **Et-CH_3**- and **Et-CH_2F**-LVs, which showed strong gene-silencing effect, was similar to that of **Di-CF_3**-LV at pH 7.4.

Table 2. K_d values of polyamine liposomes

	pH 7.4	pH 5.5		pH 7.4	pH 5.5
Et-CH_3	1.27 μM	1.71 μM	Di-CH_3	327 nM	24.3 nM
Et-CH_2F	2.43 μM	273 nM	Di-CH_2F	581 nM	75.0 nM
Et-CHF_2	N.D.	1.58 μM	Di-CHF_2	111 nM	41.6 nM
Et-CF_3	N.D.	N.D.	Di-CF_3	1.57 μM	320 nM

3.5 Effect of siRNA release time from LVs in the cytoplasm on gene-silencing

To demonstrate the effect of siRNA release time from LVs into the cytoplasm on gene-silencing, we measured siRNA release time into the cytoplasm from LVs by time-lapse imaging using a confocal laser-scanning microscope (**Figure 4**, **Figure S8**, **Movie S1-S8**.). FITC-conjugated siRNA was used for the experiment, and each sLV-CPP was used to transfect HT1080 cells. Then, siRNA-releasing time into the cytoplasm (siRNA-spreading throughout the cytoplasm) was recorded for the first 10 cells up to 24 h after the transfection (**Figure 4A**). **Et-CH_3**-LVs-CPP showed the fastest siRNA release (2.94 h) among the Et-LVs. Although Di-LVs showed relatively fast siRNA release compared with the Et-LVs, **Di-CF_3**-LVs-CPP had the fastest (2.05 h) among the Di-LVs. These results indicate that fast siRNA release from the nanocarriers is important for the effective gene-silencing. To elucidate the relationship between proportion of siRNA-diffusing cells and gene-silencing effect, the proportion of cells with siRNA that had diffused throughout the cytoplasm at a selected time point was measured (**Figure 4B**). The diffusion of siRNA was observed in about 70% of cells 24 h after the transfection with **Et-CH_3-** or **Di-CF_3**-LV-CPPs. However, proportion of siRNA-diffused cells was less than 10% for the other LV-CPPs. siRNA delivered by LVs containing **Et-CH_2F**, **Et-CHF_2** or **Et-CF_3** did not spread out in the cytoplasm, but remained in a compact form and appeared to have difficulty escaping from the endosomes because of low pK_a. Therefore, the diffusion of siRNA might not be observed. Since the interaction of siRNA to LVs containing **Et-CH_3**-LVs was weak, siRNA might be immediately released from the LVs after the endosomal escape and spread into the cytoplasm. In terms of the DiETA-series, it seems that every Di-sLV-CPP could escape from the endosome because hemolytic activities of the Di-sLV-CPP were same. However, affinity of siRNA for LVs containing **Di-CF_3** was relatively weak at pH 7.4 compared with that for other Di-LVs (**Table 2**). Therefore, the **Di-CF_3**-LVs could release siRNA all over the cytoplasm effectively after the endosomal escape compared with other Di-sLV-CPPs. These results indicate that endosomal escape ability and binding affinity of siRNA for the nanocarrier are important for the siRNA spreading in the cytoplasm. High proportion of siRNA-diffusing cells should show high gene-silencing effect.

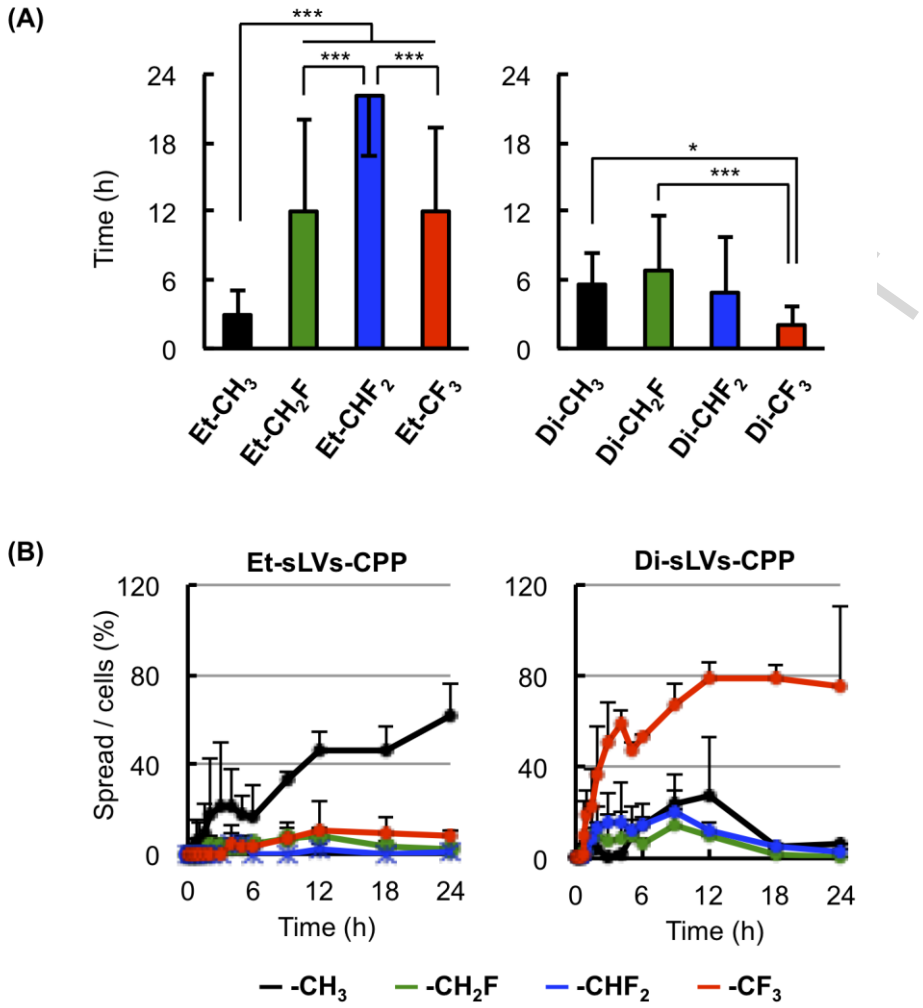

Figure 4. Intracellular behavior of siRNA delivered with LVs-CPP. HT1080 cells were transfected with FITC-siRNA-encapsulating LVs-CPP and observed by confocal laser-scanning microscopy. (A) siRNA diffusion time after transfection with LV-CPPs. Significant differences: **P*<0.05, *** *P*<0.001. (B) Proportion of siRNA-diffusing cells at selected time points. The ratio was calculated as follows: the number of FITC-distributed cells / the number of all the cells.

4. Conclusion

We succeeded in rigorous control of amine pK_a by fluorine substitution without causing a significant change in chemical structure or steric bulk. The pK_a of EtDA (mono-amine)-lipids and both pK_{a1} and pK_{a2} of DiETA (di-amine)-lipids were gently shifted to lower value by increasing the number of fluorine atoms. The optimal amine pK_a for the efficient gene-silencing depended on the number of amines. sLV-CPP containing **Et-CH_3** (pK_a = 8.2) showed a high knockdown effect in the EtDA group; and sLV-CPP containing **Di-CF_3**, (pK_{a1} = 7.1, pK_{a2} < 3.0) in the DiETA group. The hemolytic activity decreased as the pK_a in the Et-sLV-CPP decreased. However, the hemolytic activities of Di-sLVs-CPP were not changed with the fluorine atom number. The binding affinity of siRNA for the LVs changed even if the LVs showed similar surface charge and hemolytic activity. LVs having a high RNAi efficiency might be superior in the cytoplasmic release of siRNA. Moderate interaction between siRNA and nanocarrier was important for effective gene-silencing. Because sLV-CPP containing **Et-CH_3** or **Di-CF_3** showed fast siRNA release time from LVs in the cytoplasm and high proportion of siRNA-diffusing cells compared with other sLVs. Since cellular uptake amount and intracellular behavior of liposome and siRNA may vary depending on the cancer cell lines, knockdown effect may also vary according to cell lines. Therefore, adequate pK_a for strong gene-silencing may differ depending on the cell lines. Although further examination will be needed, these results indicate that it is important to control the pK_a of the carrier accurately to achieve the ideal multifunctionalitiy of the vector. We believe that these data provide general information for the design of oligonucleotide delivery vectors and will prompt the development of novel delivery vector for practical application of oligonucleotides.

Supporting Information. Information on pK_a of amine lipids, cellular uptake, knockdown effect, cell viability, interaction of siRNA for LVs, intracellular behavior of siRNA and NMR data is available in the Supporting Information

Conflict of Interest: The authors declare no competing financial interest

Acknowledgements

This research was supported by the program Grants-in-Aid for Scientific Research from the Japan Society for the Promotion of Science. The authors thank Nippon Fine Chemical Co. for the gifts of DPPC, cholesterol, DOPE, and DSPE-PEG.

REFERENCES

[1] M. Toyoshima, H.L. Howie, M. Imakura, R.M. Walsh, J.E. Annis, A.N. Chang, J. Frazier, B.N. Chau, A. Loboda, P.S. Linsley, M.A. Cleary, J.R. Park, C. Grandori, Functional genomics identifies therapeutic targets for MYC-driven cancer, Proc Natl Acad Sci U S A, 109 (2012) 9545-9550.

[2] C.V. Pecot, S.Y. Wu, S. Bellister, J. Filant, R. Rupaimoole, T. Hisamatsu, R. Bhattacharya, A. Maharaj, S. Azam, C. Rodriguez-Aguayo, A.S. Nagaraja, M.P. Morelli, K.M. Gharpure, T.A. Waugh, V. Gonzalez-Villasana, B. Zand, H.J. Dalton, S. Kopetz, G. Lopez-Berestein, L.M. Ellis, A.K. Sood, Therapeutic silencing of KRAS using systemically delivered siRNAs, Mol Cancer Ther, 13 (2014) 2876-2885.

[3] E. Bernstein, A.A. Caudy, S.M. Hammond, G.J. Hannon, Role for a bidentate ribonuclease in the initiation step of RNA interference, Nature, 409 (2001) 363-366.

[4] S.F. Dowdy, Overcoming cellular barriers for RNA therapeutics, Nature biotechnology, 35 (2017) 222-229.

[5] K.A. Whitehead, R. Langer, D.G. Anderson, Knocking down barriers: advances in siRNA delivery, Nat Rev Drug Discov, 8 (2009) 129-138.

[6] a) T. Dewa, T. Asai, Y. Tsunoda, K. Kato, D. Baba, M. Uchida, A. Sumino, K. Niwata, T. Umemoto, K. Iida, N. Oku, M. Nango, Liposomal polyamine-dialkyl phosphate conjugates as effective gene carriers: chemical structure, morphology, and gene transfer activity, Bioconjug Chem, 21 (2010) 844-852. b) T. Asai, S.

Matsushita, E. Kenjo, T. Tsuzuku, N. Yonenaga, H. Koide, K. Hatanaka, T. Dewa, M. Nango, N. Maeda, H. Kikuchi, N. Oku, Dicetyl phosphate-tetraethylenepentamine-based liposomes for systemic siRNA delivery, Bioconjug Chem, 22 (2011) 429-435.

[7] S.C. Semple, S.K. Klimuk, T.O. Harasym, N. Dos Santos, S.M. Ansell, K.F. Wong, N. Maurer, H. Stark, P.R. Cullis, M.J. Hope, P. Scherrer, Efficient encapsulation of antisense oligonucleotides in lipid vesicles using ionizable aminolipids: formation of novel small multilamellar vesicle structures, Biochim Biophys Acta, 1510 (2001) 152-166.

[8] D.W. Bartlett, M.E. Davis, Physicochemical and biological characterization of targeted, nucleic acid-containing nanoparticles, Bioconjug Chem, 18 (2007) 456-468.

[9] B. Ghosn, S.P. Kasturi, K. Roy, Enhancing polysaccharide-mediated delivery of nucleic acids through functionalization with secondary and tertiary amines, Curr Top Med Chem, 8 (2008) 331-340.

[10] S. Toita, N. Morimoto, K. Akiyoshi, Functional cycloamylose as a polysaccharide-based biomaterial: application in a gene delivery system, Biomacromolecules, 11 (2010) 397-401.

[11] O. Boussif, F. Lezoualc'h, M.A. Zanta, M.D. Mergny, D. Scherman, B. Demeneix, J.P. Behr, A versatile vector for gene and oligonucleotide transfer into cells in culture and in vivo: polyethylenimine, Proc Natl Acad Sci U S A, 92 (1995) 7297-7301.

[12] S.M. Moghimi, P. Symonds, J.C. Murray, A.C. Hunter, G. Debska, A. Szewczyk, A two-stage poly(ethylenimine)-mediated cytotoxicity: implications for gene transfer/therapy, Mol Ther, 11 (2005) 990-995.

[13] H. Uchida, K. Miyata, M. Oba, T. Ishii, T. Suma, K. Itaka, N. Nishiyama, K. Kataoka, Odd-even effect of repeating aminoethylene units in the side chain of N-substituted polyaspartamides on gene transfection profiles, J Am Chem Soc, 133 (2011) 15524-15532.

[14] M. Jayaraman, S.M. Ansell, B.L. Mui, Y.K. Tam, J. Chen, X. Du, D. Butler, L. Eltepu, S. Matsuda, J.K. Narayanannair, K.G. Rajeev, I.M. Hafez, A. Akinc, M.A. Maier, M.A. Tracy, P.R. Cullis, T.D. Madden, M. Manoharan, M.J. Hope, Maximizing the potency of siRNA lipid nanoparticles for hepatic gene silencing in

vivo, Angew Chem Int Ed Engl, 51 (2012) 8529-8533.

[15] C.A. Alabi, K.T. Love, G. Sahay, H. Yin, K.M. Luly, R. Langer, D.G. Anderson, Multiparametric approach for the evaluation of lipid nanoparticles for siRNA delivery, Proc Natl Acad Sci U S A, 110 (2013) 12881-12886.

[16] Y. Sato, H. Hatakeyama, M. Hyodo, H. Harashima, Relationship Between the Physicochemical Properties of Lipid Nanoparticles and the Quality of siRNA Delivery to Liver Cells, Mol Ther, 24 (2016) 788-795.

[17] J. Hao, P. Kos, K. Zhou, J.B. Miller, L. Xue, Y. Yan, H. Xiong, S. Elkassih, D.J. Siegwart, Rapid Synthesis of a Lipocationic Polyester Library via Ring-Opening Polymerization of Functional Valerolactones for Efficacious siRNA Delivery, J Am Chem Soc, 137 (2015) 9206-9209.

[18] J.D. Dunitz, A. Gavezzotti, Attractions and repulsions in molecular crystals: What can be learned from the crystal structures of condensed ring aromatic hydrocarbons?, Accounts Chem Res, 32 (1999) 677-684.

[19] J. Olsen, P. Seiler, B. Wagner, H. Fischer, T. Tschopp, U. Obst-Sander, D.W. Banner, M. Kansy, K. Muller, F. Diederich, A fluorine scan of the phenylamidinium needle of tricyclic thrombin inhibitors: effects of fluorine substitution on pKa and binding affinity and evidence for intermolecular C-F...CN interactions, Org Biomol Chem, 2 (2004) 1339-1352.

[20] A.L. Bailey, P.R. Cullis, Modulation of membrane fusion by asymmetric transbilayer distributions of amino lipids, Biochemistry, 33 (1994) 12573-12580.

[21] H. Koide, A. Okamoto, H. Tsuchida, H. Ando, S. Ariizumi, C. Kiyokawa, M. Hashimoto, T. Asai, T. Dewa, N. Oku, One-step encapsulation of siRNA between lipid-layers of multi-layer polycation liposomes by lipoplex freeze-thawing, Journal of controlled release : official journal of the Controlled Release Society, 228 (2016) 1-8.

[22] W. Tai, X. Gao, Functional peptides for siRNA delivery, Adv Drug Deliv Rev, 110-111 (2017) 157-168.

[23] T. Asai, T. Tsuzuku, S. Takahashi, A. Okamoto, T. Dewa, M. Nango, K. Hyodo, H. Ishihara, H. Kikuchi, N. Oku, Cell-penetrating peptide-conjugated lipid nanoparticles for siRNA delivery, Biochemical and biophysical research communications, 444 (2014) 599-604.

[24] G. Sahay, W. Querbes, C. Alabi, A. Eltoukhy, S. Sarkar, C. Zurenko, E. Karagiannis,

K. Love, D. Chen, R. Zoncu, Y. Buganim, A. Schroeder, R. Langer, D.G. Anderson, Efficiency of siRNA delivery by lipid nanoparticles is limited by endocytic recycling, Nature biotechnology, 31 (2013) 653-658.

[25] W.H. Evans, W.G. Hardison, Phospholipid, cholesterol, polypeptide and glycoprotein composition of hepatic endosome subfractions, Biochem J, 232 (1985) 33-36.

[26] J. Huotari, A. Helenius, Endosome maturation, EMBO J, 30 (2011) 3481-3500.

[27] W.G. Light, E.T. Wei, Surface charge and hemolytic activity of asbestos, Environ Res, 13 (1977) 135-145.

[28] L. Stalder, W. Heusermann, L. Sokol, D. Trojer, J. Wirz, J. Hean, A. Fritzsche, F. Aeschimann, V. Pfanzagl, P. Basselet, J. Weiler, M. Hintersteiner, D.V. Morrissey, N.C. Meisner-Kober, The rough endoplasmatic reticulum is a central nucleation site of siRNA-mediated RNA silencing, EMBO J, 32 (2013) 1115-1127.

Figure legends

Figure 1. Synthesis of fluorine-conjugated lipids.

(A) Dicetylphosphate-ethylenediamine-CH_2R (Et-R) and (B) Dicetylphosphate-diethylenetriamine-CH_2R (Di-R) conjugates were synthesized by reductive amination.

Figure 2. Effect of the number of amines and fluorine atoms on gene-silencing.

(A) TNS was mixed with lipid vesicles in a series of buffers with pH ranging between 2 and 12. Fluorescence intensity was normalized by the TNS fluorescence value at pH 2.0. (B) HT1080-EGFP cells were transfected with siGFP-encapsulating LV-CPP. RNA interference efficiency was determined as follows: Knockdown (%) / siRNA uptake (pmol/well). Significant differences :$^{**}P<0.01$, $^{***}P<0.001$

Figure 3. Membrane-destabilizing activity of sLVs-CPP.

(A) sLVs-CPP were incubated with RBCs at 37°C for 1 h in 10 mM phosphate buffer containing 0.3 M sucrose at pH 7.4 or 5.5. After centrifugation, absorbance of leaked-hemoglobin was determined at 405 nm. (B) The ζ-potential of each sLVs-CPP in 10 mM phosphate buffer was measured. Bars with oblique line indicate the ζ-potentials of sLVs-CPP at pH 7.4. Filled bars indicate those at pH 5.5.

Figure 4. Intracellular behavior of siRNA delivered with LVs-CPP.

HT1080 cells were transfected with FITC-siRNA-encapsulating LVs-CPP and observed by confocal laser-scanning microscopy. (A) siRNA diffusion time after transfection with LV-CPPs. Significant differences: $^{*}P<0.05$, *** $P<0.001$. (B) Proportion of siRNA-diffusing cells at selected time points. The ratio was calculated as follows: the number of FITC-distributed cells / the number of all the cells.

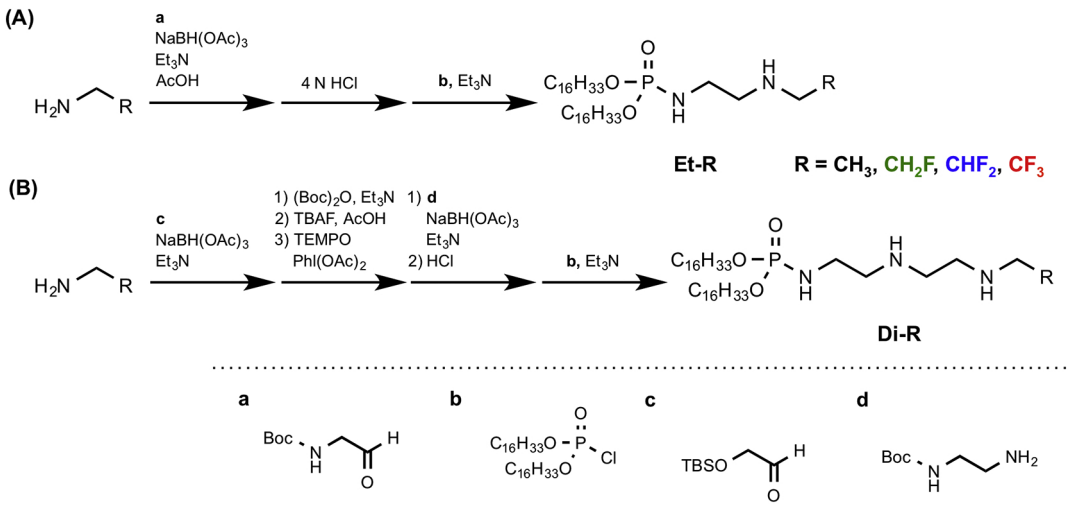
(A)
a
NaBH(OAc)3
Et3N
AcOH
4 N HCl
b, Et3N
Et-R
R = CH3, CH2F, CHF2, CF3
(B)
c
NaBH(OAc)3
Et3N
1) (Boc)2O, Et3N
2) TBAF, AcOH
3) TEMPO
PhI(OAc)2
1) d
NaBH(OAc)3
Et3N
2) HCl
b, Et3N
Di-R
a
b
c
d

Figure 1

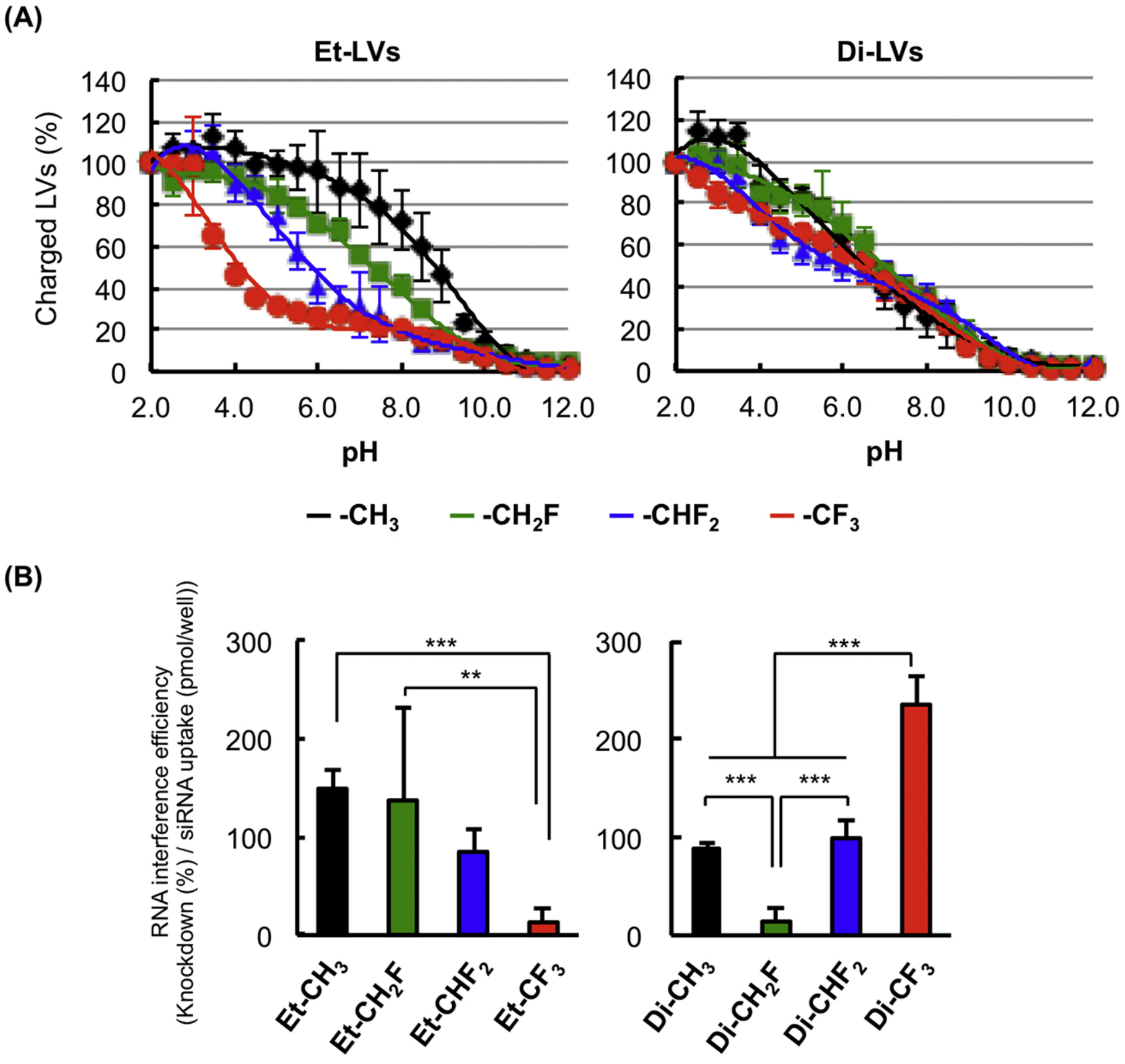
(A)
Et-LVs
Di-LVs
Charged LVs (%)
140
120
100
80
60
40
20
0
2.0
4.0
6.0
8.0
10.0
12.0
pH
-CH3
-CH2F
-CHF2
-CF3
(B)
RNA interference efficiency
(Knockdown (%) / siRNA uptake (pmol/well))
300
200
100
0
***
**
Et-CH3
Et-CH2F
Et-CHF2
Et-CF3
Di-CH3
Di-CH2F
Di-CHF2
Di-CF3

Figure 2

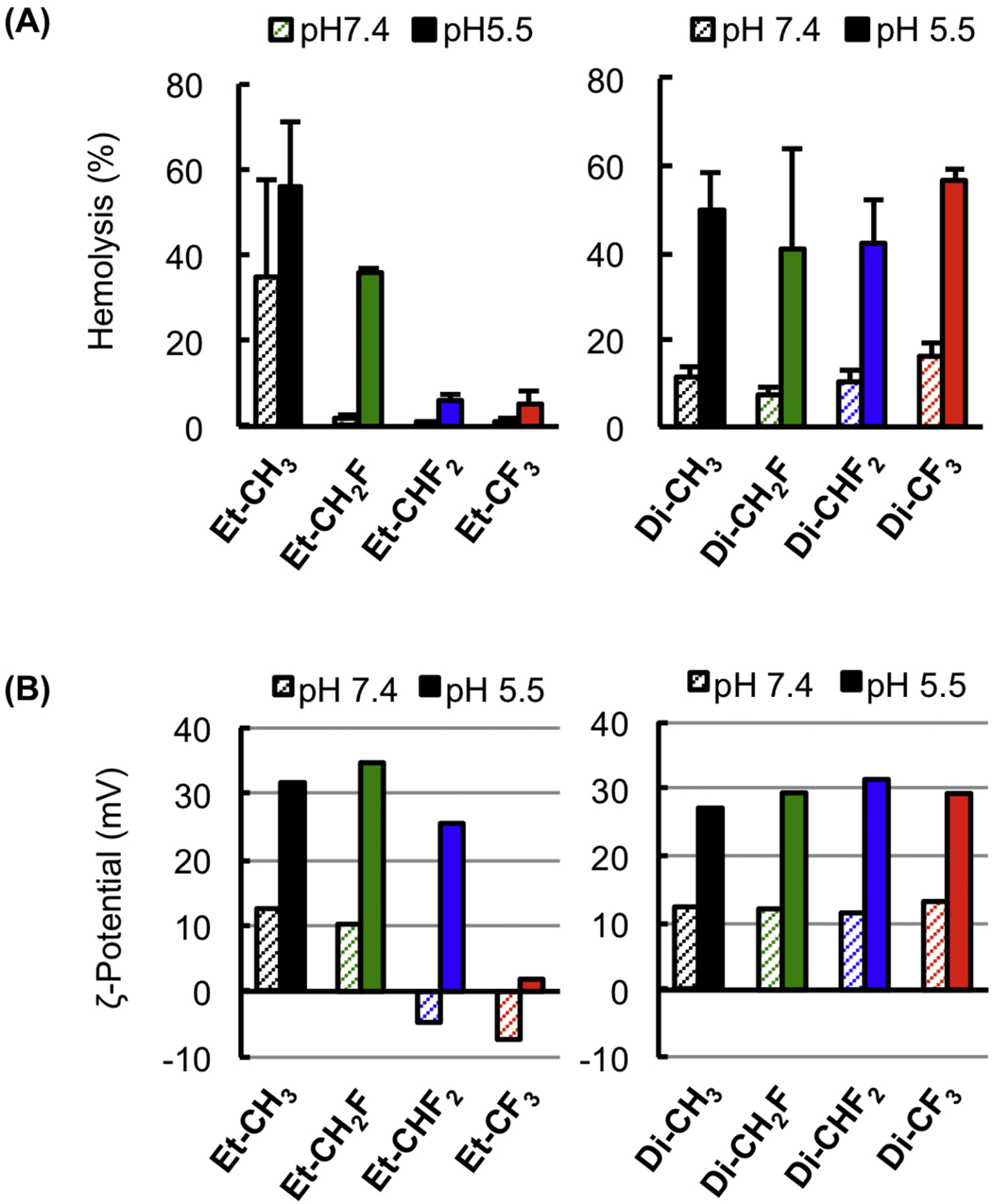
(A)
pH7.4
pH5.5
pH 7.4
pH 5.5
Hemolysis (%)
80
60
40
20
0
Et-CH3
Et-CH2F
Et-CHF2
Et-CF3
Di-CH3
Di-CH2F
Di-CHF2
Di-CF3
(B)
pH 7.4
pH 5.5
ζ-Potential (mV)
40
30
20
10
0
-10

Figure 3

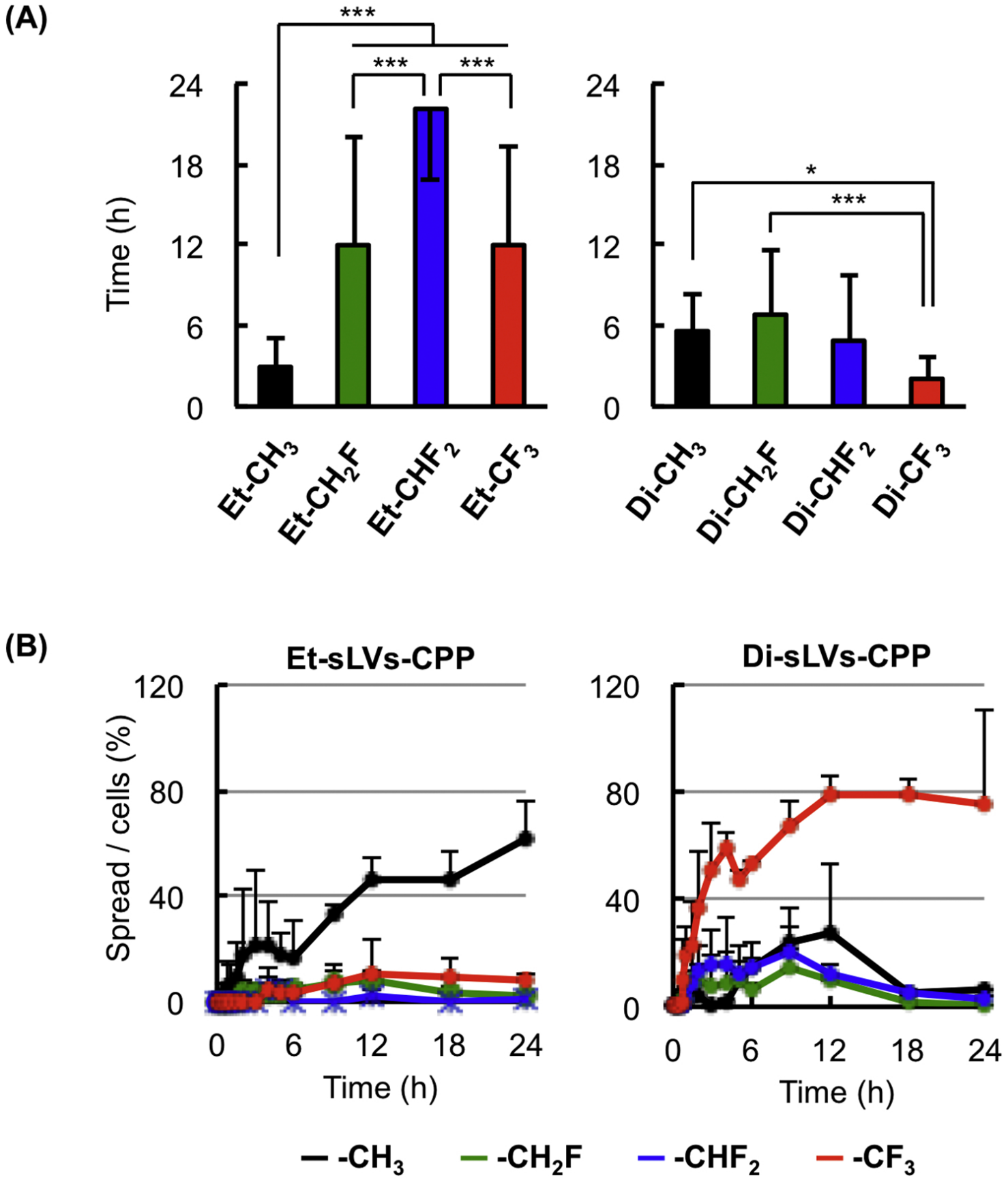
(A)
***
***
***
24
18
12
6
0
Time (h)
Et-CH3
Et-CH2F
Et-CHF2
Et-CF3
*
***
Di-CH3
Di-CH2F
Di-CHF2
Di-CF3
(B)
Et-sLVs-CPP
Di-sLVs-CPP
120
80
40
0
Spread / cells (%)
0
6
12
18
24
Time (h)
-CH3
-CH2F
-CHF2
-CF3

Figure 4